or intermolecular sulfur addition to Mo-coordinated CS_3^{2-} ligands. The latter are obtained by CS_2 addition to the Mo=S functional groups and are quite stable in the absence of available sulfur. In contrast to the Mo-η^2-CS_3 units that do not readily dissociate CS_2, the Mo-η^2-CS_4 chromophores are quite unstable in solution and readily dissociate CS_2 with formation of the Mo-η^2-S_2 units. Unlike the pronounced reactivity of "activated" alkynes such as dicarbomethoxyacetylene (DMA), which add to all available Mo=S bonds within a thiomolybdate complex, CS_2 reacts only partially. This is illustrated in the reactions of $[Mo_2S_{10/12}]^{2-}$ with these electrophilic molecules. The reaction of DMA with all, nonbridging, Mo-S_x groups in $[Mo_2S_{10/12}]^{2-}$ results in the formation of the previously reported[2] $[Mo_2S_2(S_2C_2(CO_2Me)_2)_4]^{2-}$ dithiolene complex. In contrast, the reaction with CS_2 affords III, which contains two "unreacted" Mo=S groups. At this time, we can only speculate that introduction of CS_3^{2-} or CS_4^{2-} ligands into the thiomolybdate complexes (by CS_2 addition to the Mo-S_x sites) reduces the nucleophilicity of the remaining Mo=S groups, which appear incapable of reacting further with the weakly electrophilic CS_2 molecule. The observed lack of reactivity of CS_2 with the Mo=O groups in the thiomolybdate complexes is consistent with previous studies[2,3a] of the reactions of DMA with thiomolybdate complexes and underscores the complete lack of reactivity of the Mo=O group in these complexes, at least toward electrophilic carbon sites.

At present, we are exploring the reactivity of the Mo=S and Mo—η^2-S_2 groups with other electrophiles, and in the near future, we will report[5] on the chemistry of the thiomolybdate complexes with SO_2.

Acknowledgment. The support of this work by a grant from the National Science Foundation (CHE-9006069) is gratefully acknowledged.

Supplementary Material Available: Tables S1-S5, containing listings of positional parameters, thermal parameters, and selected distances and angles of $[Ph_4P]_2[trans\text{-}(S)Mo(\eta^2\text{-}CS_4)_2]\cdot DMF$ (I), $[Ph_4P][Et_4N][cis\text{-}(S)Mo(\eta^2\text{-}CS_4)_2]$ (II), $[Ph_4P]_2[syn\text{-}cis\text{-}Mo_2(S)_2(\mu\text{-}S)_2(\eta^2\text{-}CS_4)_2]\cdot{}^1/_2DMF$ (III), $[Ph_4P]_2[syn\text{-}Mo_2(S)_2(\mu\text{-}S)_2(\eta^2\text{-}CS_3)_2]$ (IV), and $[Et_4N]_2[Mo_2(O)_2(\mu\text{-}S)_2(\eta^2\text{-}CS_4)(\eta^2\text{-}CS_3)]$ (V) (41 pages); Tables S6-S9, listing calculated and observed structure factors for I, IV, V, and II (116 pages). Ordering information is given on any current masthead page. Crystallographic data for the $[Ph_4P]_2[syn\text{-}cis\text{-}Mo_2(S)_2(\mu\text{-}S)_2(\eta^2\text{-}CS_4)_2]\cdot{}^1/_2DMF$ complex already have been deposited with a previous communication.[4]

Contribution from the Institut für Physikalische und Theoretische Chemie and Physikalisches Institut, University of Erlangen-Nürnberg, D-8520 Erlangen, Germany, and Department of Chemistry, University of Surrey, Guildford GU2 5XH, Great Britain

Rapid versus Intermediate Electronic Relaxation between $S = {}^3/_2$ and $S = {}^1/_2$ States in Nitrosyl-Iron Complexes with Jäger-Type Ligands

E. König,*[,1] G. Ritter,[2] J. Dengler,[2] and L. F. Larkworthy[3]

Received April 15, 1991

The spin-state transitions between low-spin ($S = {}^1/_2$) and intermediate-spin ($S = {}^3/_2$) states in the complexes [Fe(J·ph)NO] and [Fe(J·mph)NO] with Jäger-type ligands have been studied between 80 and 320 K on the basis of magnetism, ^{57}Fe Mössbauer effect, and X-ray powder diffraction. The transition in [Fe(J·ph)NO] is centered at $T_c \simeq 143$ K, the electronic relaxation between the spin states being rapid with $\tau \lesssim 1 \times 10^{-8}$ s at all temperatures. The transition in [Fe(J·mph)NO] is centered at $T_c \simeq 187$ K, the line shapes of the Mössbauer spectra being reproduced by a stochastic two-state relaxation model. The dynamics of the transition are determined by values of the rate constant k_{IL} between 4.31×10^6 and 6.09×10^6 s^{-1}. The temperature dependence is described by an Arrhenius equation with the activation energies $\Delta E_{IL} = 0.32$ kJ mol^{-1} and $\Delta E_{LI} = 4.23$ kJ mol^{-1} for the IS → LS and LS → IS conversion, respectively. The corresponding frequency factors are $A_{IL} = 6.9 \times 10^6$ s^{-1} and $A_{LI} \sim 63.7 \times 10^6$ s^{-1}. Shifts of the peak profiles of X-ray diffraction depend linearly on μ_{eff}^2 showing that the transition is closely associated with a modification of unit cell dimensions.

Introduction

Nitrosyl iron complexes [Fe(J·R)NO] where H_2(J·R) denotes a quadridentate Jäger-type ligand[4] have been reported by Numata et al.[5] On the basis of magnetic studies over the temperature range 80-300 K, it was suggested that the two complexes where R = ph and mph (ph = *o*-phenylene, mph = 4-methyl-*o*-phenylene) are involved in a spin-state transition. According to the data, the transition appears to be of the continuous type.

Spin-state transitions between intermediate-spin (IS, $S = {}^3/_2$) and low-spin (LS, $S = {}^1/_2$) states in mononitrosyl iron complexes have been reported previously. The transition in [Fe(salen)NO] where H_2salen = *N*,*N*′-ethylenebis(salicylideneamine) occurs at $T_c = 175$ K and shows a discontinuous character.[6,7] The structure changes associated with the transition are moderate. Studies[8] at 296 and 98 K demonstrate that the average distance between the Fe atom and the N atoms of the salen ligand as well as the distance between Fe and the mean plane of the coordinating N and O atoms decreases by about 0.10 Å in the course of the IS → LS conversion. Simultaneously, the Fe-N-O bond angle decreases from 147 to 127°. Individual Mössbauer spectra corresponding to the $S = {}^3/_2$ and $S = {}^1/_2$ states have been observed. Consequently, the transition is slow on the Mössbauer effect time scale, the relaxation time for the spin conversion being greater than about 1×10^{-7} s. The spin-state transition in the analogous [Fe(salphen)NO] where H_2salphen = *N*,*N*′-*o*-phenylenebis(salicylideneamine) occurs at $T_c \simeq 181$ K, the electronic relaxation between the two spin states being rapid with a relaxation time $\tau \lesssim 1 \times 10^{-8}$ s.[9-11] A

(1) Institut für Physikalische und Theoretische Chemie, University of Erlangen-Nürnberg.
(2) Physikalisches Institut, University of Erlangen-Nürnberg.
(3) University of Surrey.
(4) Wolf, L.; Jäger, E. G. *Z. Anorg. Allg. Chem.* **1966**, *346*, 76.
(5) Numata, Y.; Kubokura, K.; Nonaka, Y.; Okawa, H.; Kida, S. *Inorg. Chim. Acta* **1980**, *43*, 193.
(6) Earnshaw, A.; King, E. A.; Larkworthy, L. F. *J. Chem. Soc. A* **1969**, 2459.
(7) Wells, F. V.; McCann, S. W.; Wickman, H. H.; Kessel, S. L.; Hendrickson, D. N.; Feltham, R. D. *Inorg. Chem.* **1982**, *21*, 2306.
(8) Haller, K. J.; Johnson, P. L.; Feltham, R. D.; Enemark, J. H.; Ferraro, J. R.; Basile, L. J. *Inorg. Chim. Acta* **1979**, *33*, 119.
(9) Fitzsimmons, B. W.; Larkworthy, L. F.; Rogers, K. A. *Inorg. Chim. Acta* **1980**, *44*, L 53.
(10) König, E.; Ritter, G.; Waigel, J.; Larkworthy, L. F.; Thompson, R. M. *Inorg. Chem.* **1987**, *26*, 1563.

0020-1669/92/1331-1196$03.00/0

rapid transition between the $S = {}^3/_2$ and $S = {}^1/_2$ states has also been found in $[Fe(TMC)NO](BF_4)_2$ where TMC = 1,4,8,11-tetramethyl-1,4,8,11-tetraazacyclotetradecane (tetramethylcyclam).[12] However, this complex is rather dissimilar to the previous two, its geometry being intermediate between a square pyramid and a trigonal bipyramid with a nearly linear FeNO group, whereas [Fe(salen)NO] is characterized by a molecular structure close to tetragonal pyramidal and a bent FeNO group (average angle 147° in the IS state).[8]

The present investigation has been initiated in order to obtain a more detailed characterization of the spin-state transitions in the nitrosyl-iron complexes [Fe(J·ph)NO] and [Fe(J·mph)NO] of Numata et al.[5] Although structural information on these two complexes is lacking, a detailed physical description of the transitions is highly desirable in view of the very few available examples of spin-state transitions in nitrosyl-iron complexes.

The study is a further contribution within our program to define the physical nature and the mechanism of spin-state transitions in more detail.[13-15]

Experimental Section

Compound Preparation. The ligands H_2(J·ph), *N,N'-o*-phenylenebis(3-hydroxy-2-acetyl-but-2-enimine, and H_2(J·mph), its 4-methyl derivative, were synthesized according to the method described by Wolf and Jäger.[4] The molecular structure of the complex [Fe(J·ph)NO] is

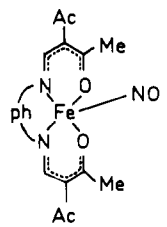

[Fe(J·ph)NO]. The compound was prepared following the procedure of Numata et al.[5] from iron(II) perchlorate hexahydrate. To this end, 0.83 g (2.3×10^{-3} mol) of iron(II) perchlorate hexahydrate was dissolved in deoxygenated methanol (15 mL). To this were added 0.75 g (2.3×10^{-3} mol) of H_2(J·ph) and 0.38 g (4.6×10^{-3} mol) of anhydrous sodium acetate in about 10 mL of methanol. The mixture was stirred at 70–80 °C for several hours and then allowed to cool overnight. The solvent was decanted from the brown needles of Fe(J·ph) which had separated. Methanol (20 mL) was then added to the Fe(J·ph), the nitrogen removed, and nitric oxide admitted. The reaction flask was connected to a gas buret and on stirring the volume of NO absorbed corresponded approximately to one mole of gas to one mole of iron(II) added as perchlorate. The brown precipitate which separated was filtered off, washed with cold deoxygenated methanol and dried in vacuo. Anal. Calcd for $C_{18}H_{18}N_3O_5Fe$: C, 52.45; H, 4.40; N, 10.19. Found: C, 52.59; H, 4.56; N, 10.53. The infrared spectrum contains absorption bands due to ν(NO) at 1790 and 1710 cm^{-1}.

[Fe(J·mph)NO]. The compound was prepared according to the procedure described by Numata et al.[5] using methanol instead of CH_2Cl_2 as the solvent. Anal. Calcd for $C_{19}H_{20}N_3O_5Fe$: C, 53.54; H, 4.73; N, 9.86. Found: C, 54.52; H, 5.00; N, 9.92. The infrared spectrum contains absorption bands due to ν(NO) at 1780 and 1700 cm^{-1}.

Physical Measurements. The ^{57}Fe Mössbauer spectra were measured with a spectrometer consisting of a constant-acceleration electromechanical drive and a Nuclear Data ND 2400 multichannel analyzer operating in the multiscaling mode. The source consisted of 50-mCi ^{57}Co in rhodium at room temperature, the calibration being effected with a 25-μm iron foil absorber. All velocity scales and isomer shifts are referred to the iron standard at 298 K. For conversion to the sodium nitroprusside scale, add +0.257 mm s^{-1}. Variable-temperature measurements between 80 and 300 K were performed by using a custom-made cryostat, the temperature being monitored by means of a calibrated iron vs constantan thermocouple and a cryogenic temperature controller (Thor Cryogenics Model E 3010-II). The areas of all spectra were corrected for the nonresonant background of the γ-rays, and the Mössbauer spectra of [Fe(J·ph)NO] were least-squares fitted to Lorentzian line shapes.

For the compound [Fe(J·mph)NO], the Mössbauer spectra were evaluated in three steps:[16] (i) Since only two lines are observed over the complete temperature range, all spectra were fitted by two independent Lorentzians (fast relaxation limit). However, the line widths of both lines are found to be excessive in the intermediate temperature range (enlargement $\simeq$45% for the left line, $\simeq$20% for the right line). The assumption of fast relaxation is therefore not applicable. (ii) The spectra at low temperatures were fitted by two symmetrical quadrupole doublets with equal line widths (slow relaxation limit). Again a significant increase of line widths is found for increasing temperatures thus showing that this simple case is not a realistic assumption. (iii) A simplified stochastic relaxation model[17,18] was applied in order to describe correctly the situation between the slow relaxation ($\tau \geq 1 \times 10^{-5}$ s) and the fast relaxation ($\tau \leq 1 \times 10^{-8}$ s) limits over the complete range of temperature. The procedure of this fit will be considered in some detail below. In contrast to a preliminary report,[16] the transmission integral consisting of the convolution of the absorber and the source function has been used in order to further improve the quality of the calculation.

Magnetic susceptibilities were measured in sealed tubes by the Gouy method over the temperature range 80–300 K. Effective magnetic moment values were calculated from the molar magnetic susceptibility χ_m according to $\mu_{eff} = 2.828(\chi_m T)^{1/2}$. The diamagnetic corrections applied to the J·ph and J·mph complexes were -156×10^{-6} and -153×10^{-6} cgsu, respectively.

Measurements of X-ray powder diffraction at variable temperatures were obtained with a Siemens counter diffractometer equipped with an Oxford Instruments CF 108A flow cryostat and liquid nitrogen as coolant.

Stochastic Two-State Relaxation Model

For the complex [Fe(J·mph)NO], significant deviations of the theoretical spectra, such as excessive line widths, are observed, if the calculations are based on a two-line (i) or a two-doublet (ii) fit. These deviations are attributed to the dynamics of the spin-state transition.

The problem of a molecule of an iron complex fluctuating between two different spin states, e.g. high-spin (HS) and low-spin (LS) states, may be conveniently described by a time-dependent Hamiltonian. To this end, a random function of time $f(t)$ is introduced, which can assume only two possible values, ± 1. For convenience of presentation we assume that the electric field gradients (efg) of the two states refer to the same principal axis system and are of axial symmetry. The resulting perturbation Hamiltonian may then be written[17]

$$H(t) = H_0 + \frac{1}{2}\left[\frac{1}{6}\Delta E_Q^{L}(3I_z^2 - I^2) + IS_L\right](1 + f(t)) + \frac{1}{2}\left[\frac{1}{6}\Delta E_Q^{H}(3I_z^2 - I^2) + IS_H\right](1 - f(t)) \quad (1)$$

In eq 1 it is

$$\Delta E_Q^{i} = \frac{eQ|V_{zz}^{i}|}{2}\,\mathrm{sign}\,(V_{zz}^{i}) \quad (2)$$

ΔE_Q^{H} and ΔE_Q^{L} being the quadrupole splitting of the HS and the LS state, respectively. In addition, IS_H and IS_L are the corresponding isomer shifts of I and I_z are the nuclear spin operators.

The Mössbauer spectra resulting from this situation are obtained by the stochastic theory of line shape, which has been developed by Blume and Tjon.[19,20] According to the theory, the probability for the absorption of a photon is determined by the quantity

$$G_{geg'e'}(p) = \sum_{ij} n_i \langle j|(\beta \mathbf{1} - \mathbf{W} - i\alpha \mathbf{F})^{-1}|i\rangle_{geg'e'} \quad (3)$$

(11) Leeuwenkamp, O. R.; Plug, C. M.; Bult, A. *Polyhedron* **1987**, *6*, 295.
(12) Hodges, K. D.; Wollmann, R. G.; Kessel, S. L.; Hendrickson, D. N.; Van Derveer, D. G.; Barefield, E. K. *J. Am. Chem. Soc.* **1979**, *101*, 906.
(13) König, E.; Ritter, G.; Kulshreshtha, S. K. *Chem. Rev.* **1985**, *85*, 219.
(14) König, E. *Prog. Inorg. Chem.* **1987**, *35*, 527.
(15) König, E. *Struct. Bonding (Berlin)* **1991**, *76*, 51.
(16) Dengler, J.; König, E.; Larkworthy, L. F.; Ritter, G.; Sengupta, S. K. *Hyperfine Interact.* **1990**, *56*, 1443.
(17) Maeda, Y.; Takashima, Y. *Mem. Fac. Sci. Kyushu Univ., Ser. C* **1983**, *14*, 107.
(18) Adler, P.; Spiering, H.; Gütlich, P. *Hyperfine Interact.* **1988**, *42*, 1035.
(19) Blume, M.; Tjon, J. A. *Phys. Rev.* **1968**, *165*, 446.
(20) Tjon, J. A.; Blume, M. *Phys. Rev.* **1968**, *165*, 456.

where i and j = HS and LS and n_i denotes the probability to find the system in state i. Moreover, **1** is the unity matrix, **W** the matrix of transition probabilities per unit time, and **F** the matrix where the diagonal elements are the permitted values of $f(t)$. In addition

$$\alpha = \pm\frac{1}{4}(\Delta E_Q{}^H - \Delta E_Q{}^L) + \frac{1}{2}(\delta_H{}^{IS} - \delta_L{}^{IS})$$

$$\beta = -i\left[\hbar(\omega - \omega_0) \mp \frac{1}{4}(\Delta E_Q{}^H + \Delta E_Q{}^L) - \frac{1}{2}(\delta_H{}^{IS} + \delta_L{}^{IS})\right] + \frac{1}{2}\Gamma_0 \quad (4)$$

where Γ_0 is the natural line width and ω_0 is the frequency of the unsplit line $\hbar\omega_0 = E_e - E_g = 14.4$ keV. The indices e,e′ and g,g′ refer to the excited and ground states, respectively, since

$$H_0|I_g m_g\rangle = E_g|I_g m_g\rangle$$
$$H_0|I_e m_e\rangle = E_e|I_e m_e\rangle \quad (5)$$

In the present case of a two-state relaxation model, the probability for transition from the HS to the LS state W_{HL} may be associated with the rate constant k_{HL} and similarly W_{LH} may be associated with the rate constant k_{LH}. If the fluctuations are described by a stationary Markoff process, the diagonal elements of matrix **W** are given by

$$W_{LL} = -k_{LH} \qquad W_{HH} = -k_{HL} \quad (6)$$

The nondiagonal elements conform to the requirement of detailed balance

$$n_H k_{HL} = n_L k_{LH} = (1 - n_H)k_{LH} \quad (7)$$

where n_H and n_L are the HS and the LS fractions, respectively. The complete matrix $(\beta\mathbf{1} - \mathbf{W} - i\alpha\mathbf{F})$ thus assumes the simple form

$$\mathbf{G}_{ge} = \begin{pmatrix} p + i\hbar\omega_L{}^{ge} + k_{LH} & -k_{LH} \\ -k_{HL} & p + i\hbar\omega_H{}^{ge} + k_{HL} \end{pmatrix} \quad (8)$$

Here, $\hbar\omega_L{}^{ge}$ and $\hbar\omega_H{}^{ge}$ are the hyperfine energies given by

$$\hbar\omega_L{}^{ge} = \delta_L{}^{IS} \pm \frac{1}{2}\Delta E_Q{}^L$$
$$\hbar\omega_H{}^{ge} = \delta_H{}^{IS} \pm \frac{1}{2}\Delta E_Q{}^H \quad (9)$$

In addition, $p = \Gamma_0/2 - i\hbar(\omega - \omega_0)$ and $\delta_i{}^{IS} = IS_i(I_e) - IS_i(I_g)$ where i = L, H. Matrix inversion of eq 8 and summation according to eq 3 then produce the final expression

$$G_{ge}(p) = [n_H(p + i\hbar\omega_L{}^{ge} + k_{LH} + k_{HL}) + n_L(p + i\hbar\omega_H{}^{ge} + k_{HL} + k_{LH})]/[(p + i\hbar\omega_H{}^{ge} + k_{HL})(p + i\hbar\omega_L{}^{ge} + k_{LH}) - k_{HL}k_{LH}] \quad (10)$$

There are thus only two different values for $G_{ge}(p)$, which will be denoted G_+ and G_-. The cross section for the absorption process of the Mössbauer effect is then determined as

$$\sigma(\omega) = \Gamma\sigma_0(\mathrm{Re}\ (G_+ + G_-))/2 \quad (11)$$

where σ_0 denotes the cross section at resonance. From this quantity, the Mössbauer spectrum can be calculated by convolution of the absorber and the source function. In order to account for possible line-broadening effects caused by instrumental factors, a line width $\Gamma_s = 0.22$ mm s^{-1} was used for all spectra. For the quantity Γ in eq 11 of the cross section, the natural line width $\Gamma_0 = 0.097$ mm s^{-1} has always been used.

In the present case, some additional assumptions have to be introduced in order to make the calculations practicable. Thus it has been assumed that the Debye–Waller factors for the two states are equal. Indeed, for the fast relaxation limit (model i), it has been shown[16] that the effective thickness t_{eff} calculated from the area is well reproduced within the high-temperature approximation of the Debye model, a single Debye temperature ($\Theta_D \simeq 123$ K for $M = 57$ au) being applicable for both spin states. It follows that the Debye–Waller factors of both spin states are equal within experimental uncertainty. Finally, in order to determine the quantity $G_{ge}(p)$ of eq 10, values of the IS fraction n_{IS} are required. These data have been obtained[16] from the numerical fit in the slow relaxation limit (model ii) as $n_{IS} = t_{eff}{}^{IS}/(t_{eff}{}^{IS} + t_{eff}{}^{LS})$. It has been verified that the derived values of n_{IS} are linearly correlated to $\mu_{eff}{}^2$, the effective magnetic moment squared, the extrapolation to $n_{IS} = 1.0$ and $n_{IS} = 0$ giving the values $\mu_{eff} = 3.86\ \mu_B$ and $\mu_{eff} = 1.51\ \mu_B$, which are close to the respective spin-only magnetic moments.

Table I. Magnetic Data for [Fe(J·ph)NO]

T, K	$10^6\chi_m$,[a] cgsu mol^{-1}	μ_{eff},[b] μ_B	T, K	$10^6\chi_m$,[a] cgsu mol^{-1}	μ_{eff},[b] μ_B
293	5395	3.56	140	6490	2.70
263.5	5930	3.54	136	6023	2.56
232	6635	3.51	130	5505	2.39
199.5	7535	3.47	126	5225	2.29
185.5	8061	3.46	120	5047	2.20
175.5	8299	3.41	116.5	4877	2.13
167	8443	3.36	110	4767	2.05
165.5	8520	3.36	104	4758	1.99
155.5	8655	3.28	96.5	4843	1.93
145.5	7968	3.04	88.5	4970	1.88
142	6906	2.80			

[a] Molecular weight $M = 412.2$ au; diamagnetic correction $\chi_m{}^{dia} = -156 \times 10^{-6}$ cgsu mol^{-1}. [b] $\mu_{eff} = 2.828(\chi_m T)^{1/2}$, with experimental uncertainty approximately $\pm 0.05\ \mu_B$.

Table II. Magnetic Data for [Fe(J·mph)NO]

T, K	$10^6\chi_m$,[a] cgsu mol^{-1}	μ_{eff},[b] μ_B	T, K	$10^6\chi_m$,[a] cgsu mol^{-1}	μ_{eff},[b] μ_B
289	4724	3.32	165	4835	2.52
261	4971	3.22	133	4778	2.25
229	5019	3.03	101	5127	2.03
197	4985	2.80	87	5653	1.98

[a] Molecular weight $M = 426.2$ au; diamagnetic correction $\chi_m{}^{dia} = -153 \times 10^{-6}$ cgsu mol^{-1}. [b] $\mu_{eff} = 2.828(\chi_m T)^{1/2}$, with experimental uncertainty approximately $\pm 0.05\ \mu_B$.

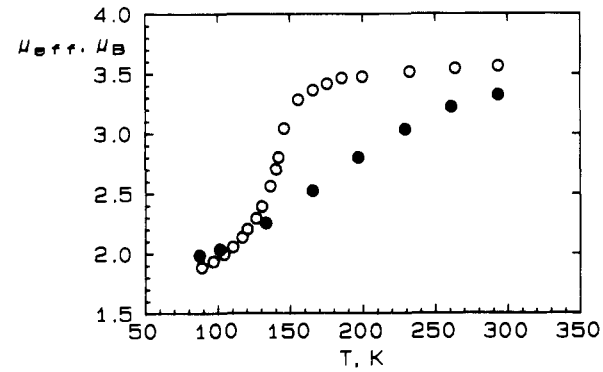

Figure 1. Temperature dependence of the effective magnetic moment μ_{eff} for [Fe(J·ph)NO] (○) and [Fe(J·mph)NO] (●).

Results

Magnetism. The magnetic data for the complexes [Fe(J·ph)NO] and [Fe(J·mph)NO] are listed in Tables I and II, respectively, their temperature dependence being displayed, in terms of the effective magnetic moment, in Figure 1. It is evident that, for [Fe(J·ph)NO], the magnetic moment decreases gradually from the value $\mu_{eff} = 3.56\ \mu_B$ at 293 K to $\mu_{eff} = 1.88\ \mu_B$ at 88.5 K. The decrease is even more gradual for [Fe(J·mph)NO] where the change is from $\mu_{eff} = 3.32\ \mu_B$ at 289 K to $\mu_{eff} = 1.98\ \mu_B$ at 87 K.

Mössbauer Effect. For [Fe(J·ph)NO], ^{57}Fe Mössbauer spectra have been measured for 23 individual temperatures between 85.3 and 300.1 K. The Mössbauer parameters resulting from the fit of the data by two independent Lorentzians are listed in Table

Table III. ^{57}Fe Mössbauer Effect Parameters for [Fe(J·ph)NO]

T, K	ΔE_Q,[a] mm s^{-1}	δ^{IS},[b] mm s^{-1}	Γ_{left},[c] mm s^{-1}	Γ_{right},[c] mm s^{-1}
300	0.388	+0.441	0.352	0.314
270	0.379	+0.459	0.368	0.305
210	0.358	+0.485	0.353	0.312
167	0.326	+0.494	0.388	0.323
142	0.535	+0.441	0.387	0.334
137	0.764	+0.401	0.364	0.320
132	0.906	+0.382	0.349	0.311
120	1.130	+0.352	0.341	0.300
100	1.321	+0.330	0.342	0.306
85	1.398	+0.326	0.348	0.308

[a] Experimental uncertainty ±0.005 mm s^{-1}. [b] Relative to metallic iron at 298 K. Experimental uncertainty ±0.005 mm s^{-1}. [c] Experimental uncertainty ≤0.01 mm s^{-1}.

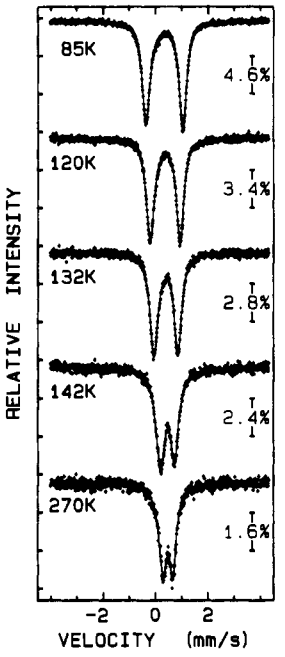

Figure 2. ^{57}Fe Mössbauer spectra of [Fe(J·ph)NO] at 85, 120, 132, 142, and 270 K. Full lines correspond to a least-squares fit by two independent Lorentzians.

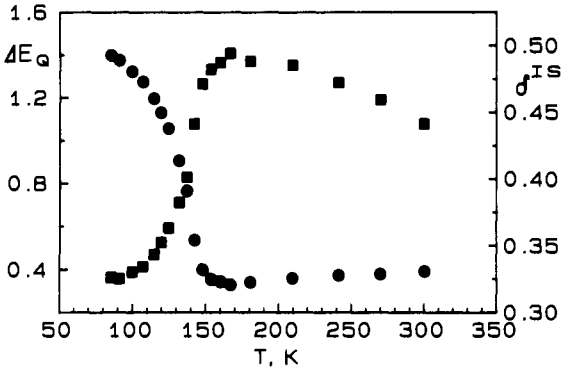

Figure 3. Quadrupole splitting ΔE_Q (●, left-hand scale) and isomer shift δ^{IS} (■, right-hand scale) of [Fe(J·ph)NO] as a function of temperature.

III for a number of representative temperatures. In addition, the spectra at 85, 120, 132, 142, and 270 K are illustrated in Figure 2. The detailed temperature dependence of the quadrupole splitting ΔE_Q and the isomer shift δ^{IS} is plotted in Figure 3. The measurements have been performed for increasing as well as decreasing temperatures, no hysteresis effects having been detected. Within experimental uncertainty, the line width Γ is practically independent of temperature as shown by the values of Table III. This indicates that the employed fitting procedure is adequate.

For the compound [Fe(J·mph)NO], the Mössbauer spectra between 84 and 319 K were reproduced by a two-state relaxation

Table IV. ^{57}Fe Mössbauer Effect Parameters for [Fe(J·mph)NO]

T, K	ΔE_Q^{IS},[a] mm s^{-1}	ΔE_Q^{LS},[a] mm s^{-1}	δ_{IS}^{IS},[b] mm s^{-1}	δ_{LS}^{IS},[b] mm s^{-1}	n_I	$10^{-6}k_{IL}$, s^{-1}
319	0.24	0.66	0.363	0.404	0.70	6.09
282	0.25	0.76	0.359	0.380	0.67	5.99
239	0.36	0.86	0.376	0.355	0.59	5.24
223	0.42	0.96	0.378	0.350	0.54	6.01
212	0.49	0.98	0.388	0.339	0.50	5.67
203	0.52	1.03	0.383	0.330	0.47	5.35
182	0.66	1.16	0.382	0.317	0.38	5.25
163	0.77	1.24	0.377	0.309	0.31	4.85
120	1.03	1.40	0.371	0.299	0.18	4.24
84	1.15	1.48	0.355	0.304	0.13	4.31

[a] Experimental uncertainty ±0.010 mm s^{-1}. [b] Relative to metallic iron at 298 K. Experimental uncertainty ±0.008 mm s^{-1}.

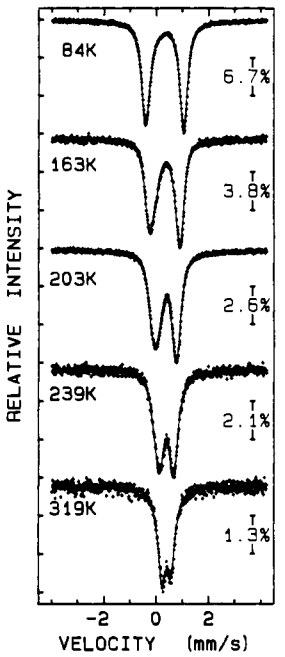

Figure 4. ^{57}Fe Mössbauer spectra of [Fe(J·mph)NO] at 84, 163, 203, 239, and 319 K. Full lines correspond to a least-squares fit based on a stochastic two-state relaxation model.

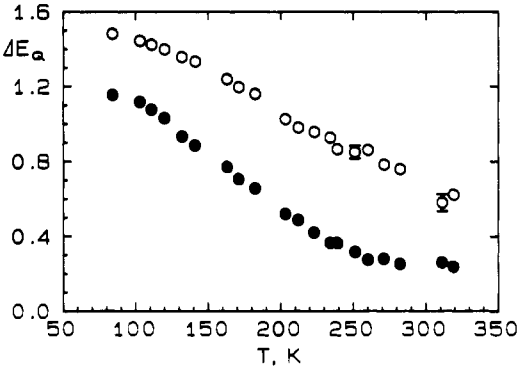

Figure 5. Quadrupole splitting ΔE_Q^{LS} for the low-spin state (○) and ΔE_Q^{IS} for the intermediate-spin state (●) of [Fe(J·mph)NO] as a function of temperature. The data are the results of the application of the stochastic two-state relaxation model.

model based on the stochastic theory of line shape. The resulting parameters are collected in Table IV, representative spectra for a number of temperatures being shown in Figure 4. The temperature dependence of the quadrupole splittings ΔE_Q for the involved spin states IS and LS is displayed in Figure 5, and that of the isomer shifts δ^{IS}, in Figure 6. The procedure for [Fe(J·mph)NO] also yields the rate constant k_{IL} for the spin-state conversion IS → LS as well as the fraction n_I of the IS state (from model ii), which are included in Table IV. These results replace

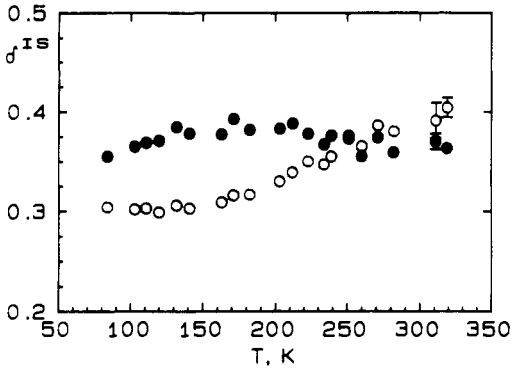

Figure 6. Isomer shift δ_{LS}^{IS} for the low-spin state (○) and δ_{IS}^{IS} for the intermediate-spin state (●) of [Fe(J·mph)NO] as a function of temperature. The data are the results of the application of the stochastic two-state relaxation model.

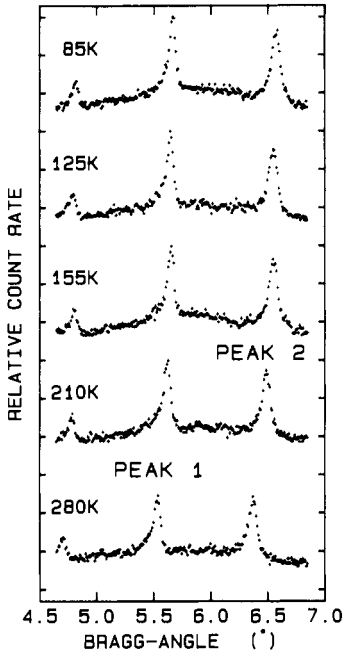

Figure 7. X-ray powder diffraction of [Fe(J·mph)NO] within the range of the Bragg angle $4.50° < \theta < 7°$ for temperatures between 89 and 280 K.

the data of a preliminary report.[16] Due to the improved evaluation procedure indicated above, the present results are considerably more accurate than the previous ones.

X-ray Diffraction. The X-ray diffraction of a powder sample of [Fe(J·mph)NO] has been measured for 16 temperatures between 78 and 290 K. The most pronounced peaks are found in the Bragg angle range 4.50–7.00°, the peak profiles for four representative temperatures being displayed in Figure 7. There is a significant shift of the peak profiles with temperature which is evident from Figure 8. In the figure, the temperature dependence of the relative d_{hkl} values for peaks 1 and 2 of Figure 7 is plotted in comparison to the ⟨111⟩ reflection of metallic Cu.

Discussion

The spin-only values for the magnetic moment of the IS ($S = {}^3/_2$) and LS ($S = {}^1/_2$) ground states of a Fe^{3+} ion are 3.87 and 1.73 μ_B, respectively. The variation of μ_{eff} values from 3.56 and 3.32 μ_B at room temperature for [Fe(J·ph)NO] and [Fe(J·mph)NO], respectively, almost to the spin-only value at 88 K suggests that a spin-state transition between these two states is involved. This is corroborated by the Mössbauer spectra for the two compounds. The magnetic moment values where the fraction of the $S = {}^3/_2$ state assumes the value $n_{IS} = 0.50$ provides an estimate for the virtual transition temperature as $T_c \simeq 143$ K for

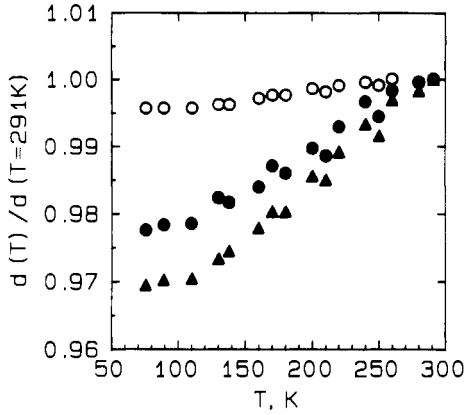

Figure 8. Relative d_{hkl} values $d(T)/d(T = 291\ K)$ for X-ray diffraction peaks 1 (●) and 2 (▲) of [Fe(J·mph)NO] and the ⟨111⟩ reflection of Cu (○) as a function of temperature.

[Fe(J·ph)NO] and $T_c \simeq 187$ K for [Fe(J·mph)NO].

As far as [Fe(J·ph)NO] is concerned, the measured Mössbauer spectra display, according to Figure 2, a unique doublet characterized by a decreasing quadrupole splitting with increasing temperature. The quadrupole doublet observed at 85 K is assigned to a $S = {}^1/_2$ state of iron on the basis of its isomer shift value $\delta^{IS} = +0.326$ mm s^{-1}, particularly if considered in conjunction with the magnetic data at the same temperature. On the other hand, the value $\delta^{IS} = +0.441$ mm s^{-1} for the Mössbauer doublet at 300.1 K is consistent with a $S = {}^3/_2$ state of iron,[21] which is suggested by the measured magnetic moment. In the temperature range between the two limits, the compound is thus involved in a spin-state transition between the IS ($S = {}^3/_2$) and LS ($S = {}^1/_2$) states. The observed unique doublet in the intermediate range of temperature is typical for a situation where the relaxation between the spin states is rapid as compared to the time scale of Mössbauer spectroscopy. Thus the Fe nucleus is influenced alone by the average of the ΔE_Q and δ^{IS} values which characterize the involved spin states. Accordingly, the relaxation time may be specified as $\tau \lesssim 1 \times 10^{-8}$ s.

The temperature dependence of the quadrupole splitting ΔE_Q shows a gradual change between the limiting values of the LS and IS states (cf. Figure 3) and is similar to that of [Fe(salphen)NO], which is also characterized by a rapid relaxation between the spin states.[10] The isomer shift for spin-invariant complexes should increase with decreasing temperature, thus reflecting the temperature dependence of the second-order Doppler shift. This is indeed observed above ~180 K for the $S = {}^3/_2$ state; cf. Figure 3. In the region of the transition, the δ^{IS} values for the $S = {}^3/_2$ and $S = {}^1/_2$ states experience a continuous transformation into each other. The behavior is similar to that of [Fe(salphen)NO] except for the considerably lower transition temperature, which is $T_c \simeq 140$ K based on the isomer shift data. The line widths Γ of the two Mössbauer lines show little temperature dependence apart from a slight irregularity in the region of the transition; cf. Table III. The temperature dependence of the total area A of the Mössbauer spectrum is similar to that of [Fe(salphen)NO][10] and demonstrates that the recoil-free fraction f is decreasing significantly on transition from the $S = {}^1/_2$ to the $S = {}^3/_2$ state. This is strong indication of a modification of unit cell dimensions or changes of metal–ligand bond lengths and bond angles at the transition or both. It is well known that spin-state transitions are in general accompanied by such changes.[14] Recently, Maeda and Takashima demonstrated[17] that, in the case of rapid relaxation, the relative sign of the efg of the two spin states may be derived from the dependence of ΔE_Q on the HS fraction n_H. Thus a linear dependence of ΔE_Q is found if both efg's have the same principal axis system and the signs of V_{zz}, the main component of the efg, are the same. For different principal axis

(21) Greenwood, N. N.; Gibb, T. C. *Mössbauer Spectroscopy*; Chapman and Hall: London, 1971.

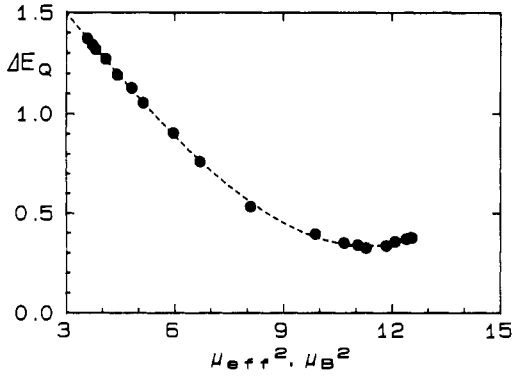

Figure 9. Quadrupole splitting ΔE_Q as a function of the effective magnetic moment squared μ_{eff}^2 for [Fe(J·ph)NO] at various temperatures. The dashed curve is a guide for the eyes.

systems and different signs, a curve showing a distinct minimum is found. In Figure 9, experimental ΔE_Q values for [Fe(J·ph)NO] are plotted versus μ_{eff}^2 for the same compound. The fraction n_I is related to μ_{eff}^2 according to

$$n_I = (\mu_{eff}^2 - \mu_L^2)/(\mu_I^2 - \mu_L^2) \qquad (12)$$

With the spin-only values $\mu_L^2 = 3\mu_B^2$ and $\mu_I^2 = 15\mu_B^2$, it follows that $n_I = {}^1/_{12}\mu_{eff}^2 - {}^1/_4$. The dependence of ΔE_Q on μ_{eff}^2 is therefore clear indication that the efg tensors of the IS and LS states have opposite signs. Different signs for V_{zz} of the HS and LS states in iron(II) spin transition complexes have been indeed found previously.[22,23]

Turning our attention to [Fe(J·mph)NO], we see that the Mössbauer spectra of this compound also show a single doublet, its quadrupole splitting being a decreasing function of temperature as is evident from Figure 4. Again the quadrupole doublet observed at 84 K may be attributed to a $S = {}^1/_2$ state of iron on the basis of its isomer shift value $\delta^{IS} = +0.317$ mm s^{-1}, whereas the doublet at 319 K, characterized by the isomer shift $\delta^{IS} = +0.394$ mm s^{-1}, suggests a $S = {}^3/_2$ state of iron.[21] This assignment is even more convincing if the direction of the change of ΔE_Q with temperature is considered and if it is taken into account that, according to the magnetic moment data (cf. Figure 1), the transformation is not completed even at 319 K. At first, the observation of a unique Mössbauer doublet with strongly changing quadrupole splitting may be taken as indication of a rapid relaxation between the spin states. However, it has been pointed out above that both a two-lines fit and a two-doublets fit produce excessive line widths. The experimental Mössbauer spectra were therefore fitted by the two-state relaxation model described above, the resulting relaxation times covering the intermediate range 0.493×10^{-7} s $\leq \tau \leq 0.201 \times 10^{-6}$ s. Satisfactory fits over the complete temperature range were achieved only if equal signs of the efg's were assumed for the two spin states IS and LS.

The temperature dependence of the quadrupole splittings ΔE_Q^{IS} and ΔE_Q^{LS} shows a gradual change with temperature (cf. Figure 5), that of the IS state being more pronounced than that of the LS state. Otherwise the variation is similar to that of ΔE_Q for [Fe(J·ph)NO]. The isomer shift of the IS state δ_{IS}^{IS} is practically independent of temperature, whereas δ_{LS}^{IS} for the LS state shows a slight increase with increasing temperature. This behavior is remarkable. It has been verified that the increase does not depend on the choice of parameter values fixed in the underlying calculational procedure. It is believed that the encountered behavior reflects particular properties of the studied spin-state transition which cannot be specified at present.

The shift of X-ray diffraction peak profiles with temperature (cf. Figure 8) shows that the spin-state transition is accompanied by at least a modification of the unit cell dimensions. If plotted versus μ_{eff}^2 the d_{hkl} values of the peaks follow a straight line. This

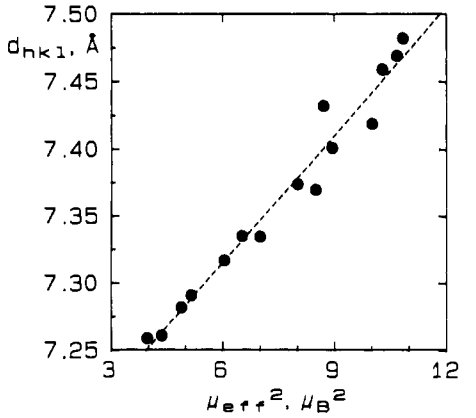

Figure 10. Values of d_{hkl} for the X-ray diffraction peak 2 of [Fe(J·mph)NO] as a function of the effective magnetic moment squared μ_{eff}^2 at various temperatures. The straight line corresponds to a least-squares fit of the data.

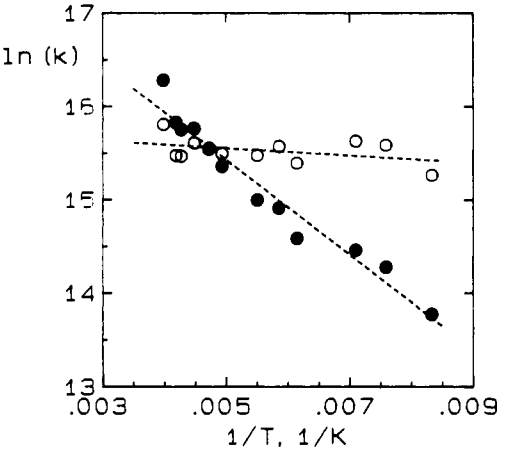

Figure 11. Arrhenius plot of ln k_{IL} (○) and ln k_{LI} (●) versus $1/T$ for [Fe(J·mph)NO]. The rate constants k_{IL} and k_{LI} for the IS → LS and LS → IS conversions, respectively, are results of application of the stochastic two-state relaxation model. The straight line corresponds to a least-squares fit of the data.

is demonstrated in Figure 10 for peak 2 of the diffraction pattern of Figure 7. The linear relationship confirms that the change of magnetic behavior and the shift of diffraction peaks are intimately related. This conclusion is consistent with results of X-ray structure studies on compounds involved in spin-state transitions.[14]

The two-state relaxation model for [Fe(J·mph)NO] also yields the rate constants for the conversion between the two spin states, the values for k_{IL} being included in Table IV. The corresponding values of the reverse rate constant k_{LI} may be obtained by application of the requirement of detailed balance eq 7 in conjunction with the values of n_I of Table IV. In the temperature range 120–251 K, the plot of ln k_{IL} or ln k_{LI} versus $1/T$ produces a straight line as illustrated in Figure 11. The kinetics of the spin-state transition may be therefore described by an Arrhenius equation

$$k = A \exp(-\Delta E/RT) \qquad (13)$$

The activation energy has been derived from the linear relation as $\Delta E_{IL} = (0.32 \pm 0.22)$ kJ mol^{-1} and $\Delta E_{LI} = (4.23 \pm 0.29)$ kJ mol^{-1}. The corresponding intercepts yield the frequency factors $A_{IL} = (6.9 \pm 1.1) \times 10^6$ s^{-1} and $A_{LI} = (63.7 \pm 12.9) \times 10^6$ s^{-1}. Using the relation

$$A \simeq e\frac{kT}{h}e^{\Delta S^*/R} \qquad (14)$$

of absolute reaction rate theory, the entropy of activation at the temperature of 200 K has been estimated as $\Delta S_{IL}^* \simeq -119$ J K^{-1} mol^{-1} and $\Delta S_{LI}^* \simeq -101$ J K^{-1} mol^{-1}, respectively. These values are within the expected range. On the other hand, the values of

(22) König, E.; Ritter, G.; Zimmermann, R.; Goodwin, H. A. *J. Chem. Phys.* **1974**, *61*, 3197.
(23) König, E.; Ritter, G.; Zimmermann, R. *Chem. Phys. Lett.* **1974**, *26*, 425.

the activation energy are rather small compared to activation energies for HS ⇌ LS transitions in complexes of iron(II).[18,24] A possible explanation may be related to the fact that Fe–ligand bond lengths in nitrosyl iron complexes decrease by about 0.1 Å on conversion from the IS to the LS state,[8] whereas changes about twice as large are encountered for HS ⇌ LS transitions in iron(II) complexes.[14]

Acknowledgment. We thank Dr. S. K. Sengupta for the preparation and magnetic measurements of [Fe(J·mph)NO]. Financial support by the Deutsche Forschungsgemeinschaft, Bonn, Germany, is gratefully acknowledged.

Registry No. [Fe(J·ph)NO], 76683-30-2; [Fe(J·mph)NO], 76683-31-3.

(24) König, E.; Ritter, G.; Dengler, J.; Nelson, S. M. *Inorg. Chem.* **1987**, *26*, 3582.

Contribution from Anorganische Chemie III, Eduard-Zintl-Institut der Technischen Hochschule Darmstadt, D-6100 Darmstadt, Federal Republic of Germany

Kinetic Studies of Nickel(II) and Copper(II) Complexes with N_4 Macrocycles of the Cyclam Type. 1. Kinetics and Mechanism of Complex Formation with Different N-Methylated 1,4,8,11-Tetraazacyclotetradecanes

Jürgen R. Röper and Horst Elias*

Received April 5, 1991

Spectrophotometry and multiscan stopped-flow spectrophotometry was used to study the kinetics of complex formation of divalent transition metal ions M^{2+} (M = Ni, Cu) with the cyclic tetraamines L^1 (=cyclam = 1,4,8,11-tetraazacyclotetradecane), L^2 = (=1-methyl-1,4,8,11-tetraazacyclotetradecane), L^3 (=1,4-dimethyl-1,4,8,11-tetraazacyclotetradecane), L^4 (=1,4,8-trimethyl-1,4,8,11-tetraazacyclotetradecane), and L^5 (=TMC = 1,4,8,11-tetramethyl-1,4,8,11-tetraazacyclotetradecane) in DMF (=*N*,*N*-dimethylformamide) at an ionic strength of 0.1 M ($NaClO_4$). Complex formation is found to be a two-step process with an initial fast second-order reaction (first-order in both $[M^{2+}]_0$ and $[L]_0$, rate constant k_1), generating an intermediate species $[ML]_{int}^{2+}$, and a subsequent slower first-order reaction (rate constant k_2), in which the intermediate is converted to the product $[ML]^{2+}$. At 303 K and for M = Ni second-order rate constant k_1 ranges from 7900 (L^1) to 61 (L^5) M^{-1} s^{-1} and follows the relative sequence 130:38:21:9:1 for L^1 to L^5, whereas first-order rate constant k_2 lies in the range 0.1×10^{-3} (L^4) to 0.9×10^{-3} s^{-1} (L^3), with the exception of $k_2(L^1) = 256 \times 10^{-3}$ s^{-1}. Even at 218 K the initial step of the reaction of Cu^{2+} ions with L^1–L^4 is too fast to be monitored by the stopped-flow technique. Complex formation of copper(II) with L^5, as studied in the temperature range 215–230 K, is also a two-step process with $k_1 = (8.70 \pm 2.60) \times 10^4$ M^{-1} s^{-1} (extrapolated value) and $k_2 = (5.40 \pm 0.03) \times 10^{-3}$ s^{-1} at 303 K. The activation parameters $\Delta H^{\ddagger}$ and $\Delta S^{\ddagger}$ for the initial fast reaction in systems Ni^{2+}/L^1–L^5 and Cu^{2+}/L^5 and for the subsequent slow reaction in systems Ni^{2+}/L^5 and Cu^{2+}/L^5 are presented. The visible spectra of the species $[ML]_{int}^{2+}$, as obtained by multiscan stopped-flow spectrophotometry, clearly indicate square-planar N_4 coordination of the tetradentate ligands L to the metal in the intermediates. Spectrophotometric titration of $[NiL^5]^{2+}$ and $[CuL^5]^{2+}$ with DMF in nitromethane at 298 K yields the equilibrium constants $K(Ni) = 0.99 \pm 0.05$ M^{-1} and $K(Cu) = 30.9 \pm 0.4$ M^{-1} for the formation of the monoadducts $[ML^5(DMF)]^{2+}$, respectively. The relative pK_a values of the species LH^+ ($pK_a(1)_r$) and LH_2^{2+} ($pK_a(2)_r$) were determined for L^1–L^5 by potentiometric titration in DMF. Increasing N-methylation ($L^1 \rightarrow L^2 \rightarrow L^3 \rightarrow L^4 \rightarrow L^5$) does not affect the size of $pK_a(1)_r$ but reduces the size of $pK_a(2)_r$. A LFE relationship exists between second-order rate constant k_1 and $pK_a(2)_r$, which suggests that formation of the second M–N bond is involved in the rate-controlling step of the formation of $[ML^{2-4}]_{int}^{2+}$. ^{1}H-NMR monitoring of the first-order reaction $[NiL^5]_{int}^{2+} \rightarrow [NiL^5]^{2+}$ proves that this step corresponds to the isomerization *RSRR*-$[NiL^5]^{2+}$ → *RSRS*-$[NiL^5]^{2+}$. It can be concluded from the size of first-order rate constants k_2 that the reactions $[ML^{1-4}]_{int}^{2+} \rightarrow [ML^{1-4}]^{2+}$ are also rearrangement reactions, in which a rapidly formed, thermodynamically less stable intermediate isomerizes via M–N bond inversion to form the more stable stereoisomer $[ML]^{2+}$.

Introduction

The fundamental importance and interdisciplinary character of the metal ion chemistry of macrocycles has recently been elegantly described and summarized by Lindoy.[1] Within the huge group of macrocyclic ligands, the aza macrocycles (and, in particular, the tetraaza macrocycles because of their possible relevance to biological systems) have attracted a great deal of attention in the past decades.[2]

A number of investigations of the rates of incorporation of metal ions such as copper(II) and nickel(II) into macrocyclic tetraamines in aqueous solution have appeared.[3] For experimental reasons these studies were carried out in acidic or alkaline media, where either protonation and solvation of the ligand or formation of hydroxo species ($Cu(OH)_3^-$ and $Cu(OH)_4^{2-}$ in the case of copper) led to problems of interpretation. To avoid these problems, Hay and Norman[4] were the first to use a dipolar aprotic solvent such as acetonitrile for the study of complex formation of nickel(II) with a series of 14-membered macrocyclic and linear N_4 ligands.

(1) Lindoy, L. F. *The Chemistry of Macrocyclic Ligand Complexes*; Cambridge University Press: Melbourne, Australia, 1989.

(2) (a) Schwind, R. A.; Gilligan, T. J.; Cussler, E. L. *Synthetic Multidentate Macrocyclic Compounds*; Academic Press: New York, 1978. (b) Melson, G. A. *Coordination Chemistry of Macrocyclic Compounds*; Plenum Press: New York, 1978. (c) Burgess, J. *Metal Ions in Solution*; Ellis Horwood Limited: Chicester, England, 1978.

(3) (a) Margerum, D. W.; Cayley, G. R.; Weatherburn, D. C.; Pagenkopf, G. K. In *Coordination Chemistry*; ACS Monograph 174; American Chemical Society: Washington, DC, 1978; Vol. 2. (b) Kaden, T. A. *Top. Curr. Chem.* **1984**, *121*, 157. (c) Leugger, A.; Hertli, L.; Kaden, T. A. *Helv. Chim. Acta* **1978**, *61*, 2296. (d) Buxtorf, R.; Kaden, T. A. *Helv. Chim. Acta* **1974**, *57*, 1035. (e) Steinmann, W.; Kaden, T. A. *Helv. Chim. Acta* **1975**, *58*, 1358. (f) Schultz-Grunow, P.; Kaden, T. A. *Helv. Chim. Acta* **1978**, *61*, 2291. (g) Hertli, L.; Kaden, T. A. *Helv. Chim. Acta* **1974**, *57*, 1328. (h) Kodama, M.; Kimura, E. *J. Chem. Soc., Dalton Trans.* **1977**, 1473. (i) Drumhiller, J. A.; Montavon, F.; Lehn, J. M.; Taylor, R. W. *Inorg. Chem.* **1986**, *25*, 3751. (j) Chen, F.-T.; Lee, C.-S.; Chung, C.-S. *Polyhedron* **1983**, *2*, 1301.

(4) Hay, R. W.; Norman, P. R. *Inorg. Chim. Acta* **1980**, *45*, L139.

0020-1669/92/1331-1202$03.00/0